Convection Heat Transfer, Entropy Generation Analysis and Thermodynamic Optimization of Nanofluid Flow in Spiral Coil Tube

Mohammadreza Kadivar[a], Mohsen Sharifpur[b,c], and Josua P. Meyer[b]

[a]Department of Mechanical and Manufacturing Engineering, Institute of Technology Sligo, Sligo, Ireland; [b]Department of Mechanical and Aeronautical Engineering, University of Pretoria, Pretoria, South Africa; [c]Institute of Research and Development, Duy Tan University, Da Nang, Vietnam

ABSTRACT

In this study, heat transfer, flow characteristics, and entropy generation of turbulent TiO_2/water nanofluid flow in the spiral coil tube were analytically investigated considering the nanoparticle volume fraction, curvature ratio, flow rate and inlet temperature between 0.01–0.05 percent, 0.03–0.06, 1.3–3.3 l/min, and 15–27 °C, respectively. Results showed that the augmentation of the nanoparticle volume fraction increased the Nusselt number and friction factor up to 11.9% and 1.1%, respectively, while it reduced the entropy generation number up to 10.9%. Reducing the curvature ratio led to a maximum of 11.1% increase in the Nusselt number, while it resulted in a 5.6% increase in the entropy generation number. A decline in the inlet temperature from 21 °C to 15 °C proceeded a 28.4% and 7.1% increase in the heat transfer and pressure drop, respectively. The total entropy generation reduced with increasing nanoparticle volume fraction. For a low Reynolds number, a decrease in the curvature ratio led to a reduction in the total entropy generation, while reducing the curvature ratio was detrimental for a high Reynolds number. Analytical relations for optimum curvature ratio and optimum Reynolds number were derived. For the range of parameters studied in this paper, a range of optimum Reynolds number from 9000 to 12,000 was proposed.

Introduction

Curved pipes have received an extensive application in industries due to their excellent heat transfer characteristics and high heat transfer coefficient in a compact structure [1, 2]. Spiral coil tube is one of the well-known types of curved tubes used widely in engineering applications, such as heat recovery processes, chemical reactors, food processing, dairy industries, refrigeration, air conditioning systems, and process industries [1–4]. The formation of secondary flow caused by the centrifugal force, cross-sectional mixing and boundary layer decoration are primary reasons for heat transfer enhancement in the curved tubes [1–3, 5].

A great deal of research interests has been devoted to nanofluids preparation, characteristics, properties, and application [6–8]. A preponderance of the heat transfer studies has used nanofluids as a working fluid [9–15]. Employing nanofluid as a working fluid improves the thermal performance of the coiled tube [1, 16, 17]. The impact of the nanofluids on the heat transfer enhancement in the curve tubes can be more effective than that of in the straight tube [18]. The increased thermal performance using nanofluids in the curved tube leads to a pressure drop penalty [3, 19–23]. Therefore, the optimization of convection heat transfer should be taken into account in the design of spiral coil tube heat exchangers. Heat transfer along a finite temperature gap and viscous effect are primary contributions of irreversibility and entropy generation in convection heat transfer [24–26]. The entropy generation analysis provides a complete identification of the source of irreversibility in the system [27–29]. As a design tool for global thermodynamic optimization, the Entropy Generation Minimization (EGM) can be employed for optimization of all kinds of heat exchangers [30].

Huminic and Huminic [1] reviewed the heat transfer and flow characteristics of conventional fluid and nanofluids in curved tubes. They reported that most of the studies in this field have devoted to the helical coil tube while the spiral coil tube has received

CONTACT Associate Professor Mohsen Sharifpur mohsen.sharifpur@up.ac.za, mohsensharifpur@duytan.edu.vn Department of Mechanical and Aeronautical Engineering, University of Pretoria, Pretoria 0002, South Africa.

Nomenclature

A_s	inside heat transfer area of the tube, m^2
B_0	heat and fluid flow "duty" parameter, $q'\dot{m}\frac{\rho}{(kT)^{1/2}\mu^{5/2}}$
Be	bejan number
C_p	specific heat capacity, J/kg K
Cr	curvature ratio
d	diameter, m
E	enthalpy, J/kg
EGM	entropy generation minimization
De	Dean number, $Re\sqrt{Cr}$
f	Darcy friction factor
h	heat transfer coefficient, W/m^2K
k	thermal conductivity, W/m K
K_b	Boltzmann's constant $(1.38066 \times 10^{-23})$, J/K
M	molecular weight, kg/mol
$\dot{m}$	mass flow rate, kg/s
N	Avogadro's number (6.022×10^{23}), 1/mol
N_s	total entropy generation number, $\frac{\dot{S}_{gen}}{(q')^2/kT^2}$
$(N_s)_T$	contribution of the entropy generation number due to heat transfer
$(N_s)_P$	contribution of the entropy generation number due to viscous effect
Nu	Nusselt number, hd_t/k
p	pressure, Pa
Pr	Prandtl number, $\mu C_p/\rho k$
q'	heat transfer rate per unit length, W/m
Q	heat transfer rate, W
R	coil radius, m
R^2	correlation coefficient
Re	Reynolds number, $\rho V d_t/\mu$
$\dot{S}_{gen}$	entropy generation rate per unit length, W/m K
s	specific entropy, W/kg K
T	temperature, K
V	velocity, m/s
x	axis in the direction of flow, m

Greek symbols

ρ	density, kg/m^3
φ	nanofluid volume fraction, %
τ	temperature difference number, $\Delta T/T$
μ	dynamic viscosity, Pa.s

Subscripts

b	bulk fluid
c	coil
LMTD	logarithmic mean temperature difference
p	nanoparticle
f	base fluid
f0	base fluid at the temperature of 293 K
fr	freezing point
h	hot water
i	initial
in	inlet
min	minimum
max	maximum
nf	nanofluid
opt	Optimum
out	outlet
t	tube

insufficient attention. Sasmito et al. [31] numerically studied the heat transfer performance of laminar Al_2O_3/water and CuO/water nanofluid flow in squared cross-section tubes with straight, spiral, conical spiral, and helical configuration. The in-plain spiral coil tube showed better thermal performance compared to the other configurations. Jamal-Abad et al. [32] experimentally recorded heat transfer and flow characteristics of laminar Al_2O_3/water and CuO/water nanofluid flow in a spiral coil tube with constant wall temperature. They showed an increase in the Nusselt number and a marginal rise in the pressure drop using nanofluid compared to that of the base fluid. They also reported that heat transfer enhancement caused by the spiral coil tube (the effect of curvature) is more than that of the addition of nanoparticle into the base fluid. Doshmanziari et al. [19, 33] conducted an experimental and numerical study to investigate the fluid flow and heat transfer characteristics of turbulent Al_2O_3/water nanofluid flow in a spiral coil tube. They reported a 60% enhancement in the convective heat transfer coefficient of the nanofluid compared to that of the base fluid. They also showed a further 14% increase in the overall performance of the spiral coil tube heat exchanger by introducing pulsation into the nanofluid flow. Naphon [34] and Naphon et al. [35] studied heat transfer and pressure drop of TiO_2/water nanofluid in a spiral coil tube under the turbulent flow condition. They showed that a decrease in the curvature ratio and an increase in the nanoparticle volume fraction leads to heat transfer enhancement and pressure drop penalty. Naphon et al. [5, 36] obtained further heat transfer enhancement in TiO_2/water nanofluid flow inside the spiral coil tube by introducing the magnetic field and pulsating flow.

Depending on the nanoparticle volume fraction, channel size, and flow regime (i.e. laminar or turbulent), a decrease in the entropy generation by adding nanoparticles was reported in a review by Mahian et al. [37]. Bianco et al. [38] studied the entropy generation of turbulent Al_2O_3/Water nanofluid flow in a tube with a squared cross-section considering constant heat flux on the wall. They found that the optimum Reynolds number reduces with increased nanoparticle volume fraction. Moghaddam et al. [39,40] investigated the entropy generation of Al_2O_3/water and Al_2O_3/EG nanofluids flow in a circular tube subjected to a constant heat flux under both laminar and turbulent flow regime. They reported that, for a given Reynolds number in laminar flow, the entropy

generation continually decreases with increasing the nanoparticle volume fraction. However, there is an optimum Reynolds number associated with turbulent flow, which decreases with increased nanoparticle volume fraction. They also found that the contribution of entropy generation due to heat transfer augments with increased Reynolds number and nanoparticle volume fraction. Leong et al. [41] estimated the entropy generation of Al_2O_3/water and TiO_2/water nanofluids in a circular tube with constant wall temperature for both laminar and turbulent flows. They demonstrated the superiority of using TiO_2 nanoparticle compared to Al_2O_3. Moreover, they indicated that increasing nanoparticle volume fraction reduces entropy generation in both laminar and turbulent nanofluid flow.

Apart from nanoparticle concentration and Reynolds number, the geometry of curved tubes influences the entropy generation [42]. Ahadi and Abbassi [43] studied entropy generation and convective heat transfer of laminar Al_2O_3/water nanofluid flow in a helical coil tube with constant wall heat flux on the tube wall. They showed that increasing the Reynolds number of the base fluid, curvature ratio, and nanoparticle volume fraction decrease the entropy generation contribution due to heat transfer and increase the entropy generation contribution caused by the viscous effect. Zamzamian [44] and Falahat [45] analyzed the entropy generation of laminar Al_2O_3/EG nanofluid flow in a helical coil tube. They showed that adding nanoparticles into the base fluid decreased the irreversibility, as long as the entropy generation caused by the viscous effect does not exceed that of due to heat transfer. Huminic and Huminic [46, 47] studied heat transfer and entropy generation of CuO/water and TiO_2/water nanofluids in helical coil tube-in-tube heat exchangers under laminar flow regime. They reported that heat transfer and entropy generation in helical coil tube-in-tube heat exchangers are dominated by nanoparticle volume fraction and nanofluid flow rate. More recently, Khosravi-Bizhaem and Abbassi [48] investigated the impact of curvature ratio on convection heat transfer and entropy generation of Al_2O_3/water nanofluid in helical coil tubes under the laminar flow regime. They reported that a low Reynolds number flow of nanofluid with a high nanoparticle volume fraction in a helical coil tube with a large curvature ratio could supply a favorable thermo-hydrodynamic performance.

According to the above literature review, nanofluid volume fraction, Reynolds number, and geometry of the curved tubes influence heat transfer, fluid flow, and entropy generation of nanofluid flow in the coiled tubes. Therefore, optimizing these parameters enhances the overall performance of coiled tube heat exchangers. A few studies have dedicated to the entropy generation of nanofluid in helical coil tubes. In contrast, the entropy generation in the spiral coil tube has received no attention so far, to the best of authors' knowledge. In a review by Yang and Du [49], the enhanced thermodynamic and heat transfer performance of TiO_2/water nanofluid, as well as good stability (with proper dispersion technique) was reported. Therefore, this study targeted the analysis of convective heat transfer and entropy generation of the TiO_2/water nanofluid in spiral coil tubes. In the upcoming sections, the impact of the curvature ratio, Reynolds number, nanofluid inlet temperature, and nanoparticle volume fraction on heat transfer, fluid flow, and entropy generation of the turbulent TiO_2/water nanofluid flow in spiral coil tubes were studied.

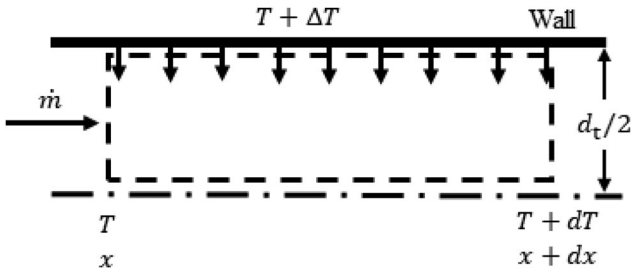

Figure 1. Schematic of the thermodynamic system.

This paper studies the effect of contributing parameters on heat transfer and pressure drop of turbulent nanofluid flow in spiral coil tubes. To find the source of the irreversibility in the heat exchanger, the entropy generation analysis is then incorporated into the study. The EGM method is also employed to optimize the convective heat transfer of the nanofluid flow in spiral coil tubes.

Analysis

Irreversibility due to heat transfer in a finite temperature gap and the viscous effect are primary sources of entropy generation in convection heat transfer [24, 25, 50]. Consider the thermodynamic system shown in Figure 1. This system is an infinitesimal passage of the coiled heat exchanger with length dx and diameter d_t in which nanofluid with a mass flow rate of $\dot{m}$ flows. The temperature gap ΔT between the tube wall and nanofluid baulk temperature, T, initiates heat transfer between the tube wall and nanofluid flow. Considering the following assumptions: the temperature gap ΔT is constant across the tube, the axial

conduction heat transfer is negligible, and nanofluid is regarded as a pure substance.

For the thermodynamic system shown in Figure 1, the first and second law of thermodynamics can be expressed as [30, 51]

$$\dot{m}\ dE = q'dx \tag{1}$$

$$\dot{S}'_{\text{gen}} = \dot{m}\frac{dE}{dx} - \frac{q'}{T+\Delta T} \tag{2}$$

where $\dot{S}'_{\text{gen}}$ and q' are the entropy generation rate and the heat transfer rate per unit length, respectively, while E is the fluid enthalpy.

Employing the thermodynamic relation

$$Tds = dE - \frac{1}{\rho}dp \tag{3}$$

where p and ρ are the pressure and the nanofluid density, respectively, and s is the fluid specific entropy, therefore, Eq. (2) can be written as

$$\dot{S}'_{\text{gen}} = \frac{\dot{m}}{\rho T}\left(-\frac{dp}{dx}\right) + \frac{\Delta T}{T^2}\frac{q'}{1+\frac{\Delta T}{T}} \tag{4}$$

The first and second terms on the right-hand side of the Eq. (4) are the contribution of entropy generation caused by the viscous effect (pressure drop) and the contribution of entropy generation due to the heat transfer, respectively. Note that the temperature difference number $\tau = \Delta T/T$ is much smaller than unity; therefore, it can be eliminated from Eq. (4) [52].

$$\dot{S}'_{\text{gen}} = \frac{\dot{m}}{\rho T}\left(-\frac{dp}{dx}\right) + \frac{q'\Delta T}{T^2} \tag{5}$$

Pressure gradient in Eq. (5) can be substituted by the Darcy-Weisbach equation

$$-\frac{dp}{dx} = \frac{2f\rho V^2}{d_t} \tag{6}$$

where f, V, and d_t are the Darcy friction factor, the flow velocity, and the tube diameter, respectively. By considering $\dot{m} = \rho V \pi {d_t}^2/4$, the pressure gradient can be written as

$$-\frac{dp}{dx} = \frac{32\dot{m}^2 f}{\rho\pi^2 {d_t}^5} \tag{7}$$

According to the definition of the convective heat transfer coefficient, $h = q'/\pi d_t \Delta T$, and Nusselt number, $Nu = hd_t/k$, the temperature gap, ΔT, can be obtained by

$$\Delta T = \frac{q'}{\pi k Nu} \tag{8}$$

By substituting Eqs. (7) and (8) into Eq. (5), the total entropy generation rate per unit length, $\dot{S}'_{\text{gen}}$, can be achieved by

$$\dot{S}'_{\text{gen}} = \frac{(q')^2}{T^2\pi k Nu} + \frac{32\dot{m}^3 f}{\rho^2\pi^2 {d_t}^5 T} \tag{9}$$

The entropy generation rate can be non-dimensionalised by $(q')^2/kT^2$ which the result is known as total entropy generation number, N_s [24].

$$N_s = \frac{\dot{S}'_{\text{gen}}}{(q')^2/kT^2} = \frac{1}{\pi Nu} + \frac{32\dot{m}^3 kTf}{\rho^2\pi^2 {d_t}^5 (q')^2} \tag{10}$$

Using the definition of the Reynolds number ($Re = 4\dot{m}/\pi d_t \mu$), Eq. (10) reduces to

$$N_s = \frac{1}{\pi Nu} + \frac{\pi^3 \mu^5 kTRe^5 f}{32\rho^2 \dot{m}^2 (q')^2} \tag{11}$$

Bejan [24, 26] defined heat and fluid flow "duty" parameter, B_0, which is an interpretation of the heat exchanger constrains ($\dot{m}$, q') and fixed by the heat exchanger design.

$$B_0 = q'\dot{m}\frac{\rho}{(kT)^{1/2}\mu^{5/2}} \tag{12}$$

Therefore, the total entropy generation number formulation reduces to

$$N_s = \frac{1}{\pi}Nu^{-1} + \frac{\pi^3}{32}Re^5 f {B_0}^{-2} \tag{13}$$

Equation (13) shows that the irreversibility of convective heat transfer in a heat exchanger depends on two dimensionless groups (Nu, f) as well as Reynolds number and the duty parameter.

Since the heat transfer rate, q', mass flow rate, $\dot{m}$, and the working fluid are specified, the objective of the entropy generation minimization is to minimize the N_s with respect to the design parameters while B_0 is constant [24].

Bejan [24] demonstrated that the optimum Reynolds number for a laminar flow in a straight duct is zero. This suggests that the diameter of the tube must be large enough to mitigate the contribution of irreversibility due to the viscous effect. For turbulent flow, however, the N_s has a unique minimum, which can be determined by minimizing the entropy generation number. Zamzamian [44] showed that, for laminar flow in a helical coil tube, increasing the Reynolds number decreases the entropy generation up to a certain Dean number. Dean number is obtained by modifying the Reynolds number with the tube curvature to consider the effect of centrifugal force caused by tube curvature. Dean number is defined as $De = Re\sqrt{Cr}$ where Cr is the tube curvature ratio. Zamzamian [44] showed that after that certain Dean

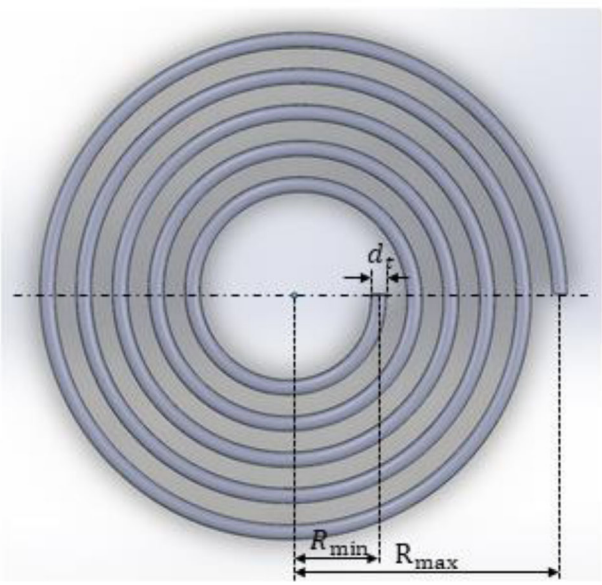

Figure 2. Geometrical features of the spiral coil tube.

number, a further increase in the Reynolds number increases the entropy generation. This suggests that there is an optimum Reynolds number for flow in curved tubes under both laminar and turbulent flow conditions. Apart from the Reynolds number, the geometry of the coiled tube can influence the entropy generation which can be minimized [34, 35, 44, 46].

Figure 2 illustrates the geometrical features of a spiral coil tube. The tube diameter and curvature ratio can characterize the geometry of a spiral coil tube. The curvature ratio is defined as the ratio of the tube's inner radius to the coil's average radius, $Cr = d_t/(R_{min} + R_{max})$, where R_{min} and R_{max} are the innermost and outermost radii the spiral coil tube, respectively.

Naphon [34] experimentally studied convection heat transfer of turbulent TiO_2/water nanofluid flow in spiral coil tubes (with a circular cross-section). The spiral coil was horizontally immersed in a hot water storage tank with a constant bath temperature. In this study, the correlations of the Nusselt number and friction factor developed by Naphon [34] were employed

$$Nu = 2.117\ Re^{0.308} Pr^{-0.077} Cr^{-0.115} \varphi^{0.068} \tag{14}$$

and

$$f = 0.268\ Re^{-0.736} Cr^{-1.042} \varphi^{0.009} \tag{15}$$

where $4000 < Re < 9000$, $4 < Pr < 7$, $0.03 < Cr < 0.06$, $0.01\% < \varphi < 0.05\%$. Naphon [34] reported that the majority of the experimental data falls within ±7.5% of the predicted results by correlations (14) and (15).

By substituting Eqs. (14) and (15) into Eq. (13), the entropy generation number for convection heat transfer of turbulent TiO_2/water nanofluid flow in spiral coil tubes reads as

$$\begin{aligned} N_s &= (N_s)_T + (N_s)_P \\ &= \left(0.150\ Re^{-0.308} Pr^{0.077} Cr^{0.115} \varphi^{-0.068}\right) \\ &\quad + \left(0.260\ Re^{4.264} {B_0}^{-2} Cr^{-1.042} \varphi^{0.009}\right) \end{aligned} \tag{16}$$

where $(N_s)_T$ and $(N_s)_P$ are the contributions of entropy generation number due to heat transfer and viscous effect, respectively. From engineering mathematics, by using the chain rule and differentiating Eq. (16) with respect to Cr, and Re, respectively, yields the general formulation for the optimum design parameters as

$$Cr_{opt} = 10.774\quad Re^{3.952} Pr^{-0.067} \varphi^{0.067} {B_0}^{-1.729} \tag{17}$$

and

$$Re_{opt} = 0.499\ Pr^{0.017} Cr^{0.253} \varphi^{-0.017} {B_0}^{0.437} \tag{18}$$

The Bejan number, Be, can be defined as the ratio of the entropy generation contribution due to heat transfer to the total entropy generation [53]

$$Be = \frac{(N_s)_T}{N_s} \tag{19}$$

The Bejan number varies between 0 and 1, where $Be = 0$ represents the irreversibility is dominated by fluid friction while $Be = 1$ denotes the domination of heat transfer in the irreversibility.

Thermophysical properties of nanofluid

Employing a suitable model for the estimation of thermophysical properties is a challenge in nanofluid modeling. Mahian et al. [54] proved that applying classical models rather than using experimental-based correlations may lead to a misprediction of the heat transfer coefficient.

Based on the physical principle of the mixture rule, Pak and Cho [55] suggested following relations for calculation of the density and heat capacity of the nanofluid, written as:

$$\rho_{nf} = \varphi\rho_p + (1 - \varphi)\rho_f \tag{20}$$

and

$$C_{p,nf} = \frac{\varphi(\rho C_p)_p + (1 - \varphi)(\rho C_p)_f}{\rho_{nf}} \tag{21}$$

where the subscripts nf, p, and f indicate nanofluid, nanoparticle, and base fluid (water), respectively.

Table 1. Thermophysical properties of TiO_2 nanoparticle [58].

d_p (nm)	ρ_p (Kg m^{-3})	$C_{p,p}$ (J Kg^{-1} K^{-1})	k_p (W m^{-1} K^{-1})
21	4170	711	11.8

Corcione [56] conducted a regression analysis using the experimental data of the thermal conductivity and viscosity of various nanofluid reported in the literature. The author established correlation (22) for the estimation of the thermal conductivity of nanofluids with a standard deviation error of 1.86%.

$$\frac{k_{nf}}{k_f} = 1 + 4.4\ Re_p^{0.4} Pr_f^{0.66} \left(\frac{T}{T_{fr}}\right)^{10} \left(\frac{k_p}{k_f}\right)^{0.03} \varphi^{0.66} \quad (22)$$

where T_{fr} is the freezing point of the base liquid and Re_p is the nanoparticle Reynolds number which is calculated by

$$Re_p = \frac{2\rho_f K_b T}{\pi \mu_f^2 d_p} \quad (23)$$

where K_b and d_p are Boltzmann's constant (1.38066×10^{-23}J/K) and the average diameter of nanoparticles, respectively. Equation (22) is valid for a nanoparticle size between 10 to 150 nm in diameter, nanoparticle volume fraction between 0.2 to 9%, and temperature between 294 and 324 K.

Corcione [56] also developed the following empirical correlation for the viscosity of nanofluid with a standard deviation error of 1.84%.

$$\frac{\mu_{nf}}{\mu_f} = \frac{1}{1 - 34.87\left(d_p/d_f\right)^{-0.3}\ \varphi^{\ 1.03}} \quad (24)$$

where d_f is the equivalent diameter of a molecule of the base fluid which is defined as

$$d_f = \left(\frac{6M}{N\pi\rho_{f0}}\right)^{1/3} = \left(\frac{6 \times 0.01801528}{6.022 \times 10^{23} \times \pi \times 998.26}\right)^{1/3} = 3.85 \times 10^{-10}\text{m} \quad (25)$$

where M, N and ρ_{f0} are the molecular weight of the base fluid, Avogadro's number, and the density of the base fluid at the temperature of 293 K, respectively. Equation (24) is valid for a nanoparticle size between 25 and 200 nm in diameter, nanoparticle volume fraction between 0.01 to 7.1%, and temperature between 293 and 333 K.

The following correlations proposed by Abbasian Arani and Amani [57] were used for estimation of the thermophysical properties of water,

The correlation for viscosity of water was proposed with a maximum deviation error of 1.2%.

Table 2. Range of the parameters.

Parameter	Minimum	Maximum
Nanoparticle volume fraction, φ (%)	0.01	0.05
Curvature ratio, *Cr*	0.03	0.06
Nanofluid temperature, *T* (°C)	15	27
Reynolds number, *Re*	4000	9000
Prandtl number, *Pr*	4	7

$$\text{Ln}\left(\frac{\mu_f}{0.001792}\right) = -1.24 - 6.44\left(\frac{273.15}{T}\right) + 7.68\left(\frac{273.15}{T}\right)^2 \quad (26)$$

The correlation of thermal conductivity of water was obtained by a curve-fitting on experimental data with a correlation coefficient of $R^2 = 99.99\%$.

$$k_f = -1.549404 + 0.01553952 \times T - 3.65967 \times 10^{-5} T^2 + 2.9401 \times 10^{-8} T^3 \quad (27)$$

The correlation of density and specific heat capacity of water were estimated with $R^2 = 99.99\%$ and $R^2 = 99.99\%$, respectively.

$$\rho_f = -764.475639 + 19.251515 \times T - 0.07714568 \times T^2 + 1.364893 \times 10^{-4} T^3 - 9.339158 \times 10^{-8} T^4 \quad (28)$$

and

$$C_{p,f} = 198531.690492 - 2894.853934 \times T + 17.2363068 \times T^2 - 0.05126994 \times T^3 + 7.616133 \times 10^{-5} T^4 - 4.517821 \times 10^{-8} T^5 \quad (29)$$

Relations (26) to (29) are valid over $273.15 \leq T \leq 373.15$ and independent of pressure.

The thermophysical properties of TiO_2 nanoparticle are listed in Table 1 [58].

All thermophysical properties were evaluated at the average bulk nanofluid temperature.

Results and discussion

Table 2 listed the range of parameters studied in this paper, which were chosen based on the limitation imposed by the correlations presented in the previous sections.

Based on Naphon's [34] study, a spiral coil tube with a tube diameter of 8.5 mm and a coil pitch of 20.5 mm was considered for this study, which was immersed in a hot water storage tank with a constant temperature. The innermost diameter of the spiral coil was considered as 94.5 mm while its outermost

diameter varied with curvature ratio. The empirical correlations proposed by Naphon [34] (Eqs. (14) and (15)) were employed for the analysis of convection heat transfer. Equations (16)–(19) were used for entropy generation analysis.

The spiral coil tube immersed in the hot water storage was considered as a heat exchanger. The temperature of the hot water bath was assumed to be 40.21 °C while the nanofluid inlet temperature varied between 15 °C to 27 °C. The thermophysical properties of TiO_2/water nanofluid were calculated using Eqs. (20)–(25). Since thermal properties require to be evaluated at the average bulk temperature of the fluid, the outlet temperature of the nanofluid flowing inside the spiral coil tube needs to be calculated. Therefore, a "trial and error" method explained in the Appendix was used for calculation of the outlet temperature. Figure 3 compares the calculated outlet temperature of the nanofluid with the experimental data by Naphon [34]. The accuracy of the Naphon's data on the temperature measurement was 0.1% [34]. Close agreement between experimental data and calculated results with an average deviation of 2.2% and a maximum deviation of 4.3%, was observed. The calculation procedure can be summarized as

1. Evaluation of the nanofluid outlet temperature, $T_{out,nf}$, using the method explained in the Appendix.
2. Calculation of the average bulk nanofluid temperature, $T_b = (T_{in,nf} + T_{out,nf})/2$.
3. Estimation of the thermo-physical properties of TiO_2 nanofluid using Eqs. (20)–(25).
4. Heat transfer analysis using Eqs. (14) and (15).
5. Entropy generation analysis employing Eq. (16).
6. EGM analysis using Eqs. (17) and (18).

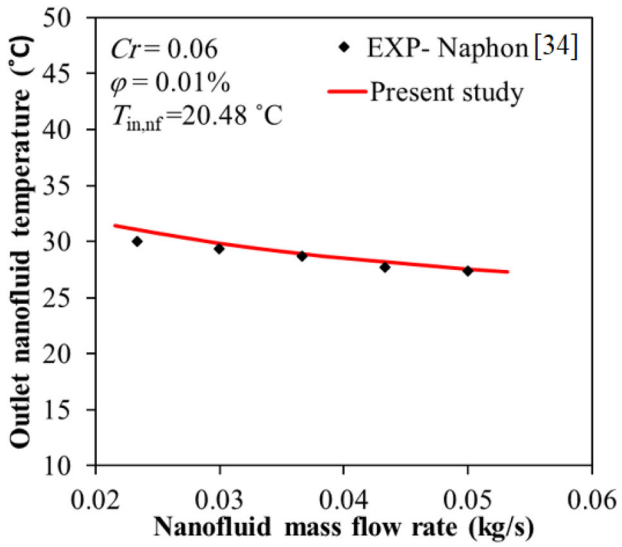

Figure 3. Comparison of calculated outlet nanofluid temperature with experimental data of Naphon [34].

Convection heat transfer

The addition of nanoparticles into the base fluid can enhance the heat transfer characteristics of the base fluid. Induced micro-convection due to Brownian motion of nanoparticles, nanoparticle migration, disruption of the thermal boundary layer, and change of thermophysical properties of the base fluid enhance transport properties of nanofluids compared to that of the base fluid [59, 60]. Figure 4 indicates the influence of nanoparticle volume fraction on the Nusselt number and friction factor of nanofluid flow in the spiral

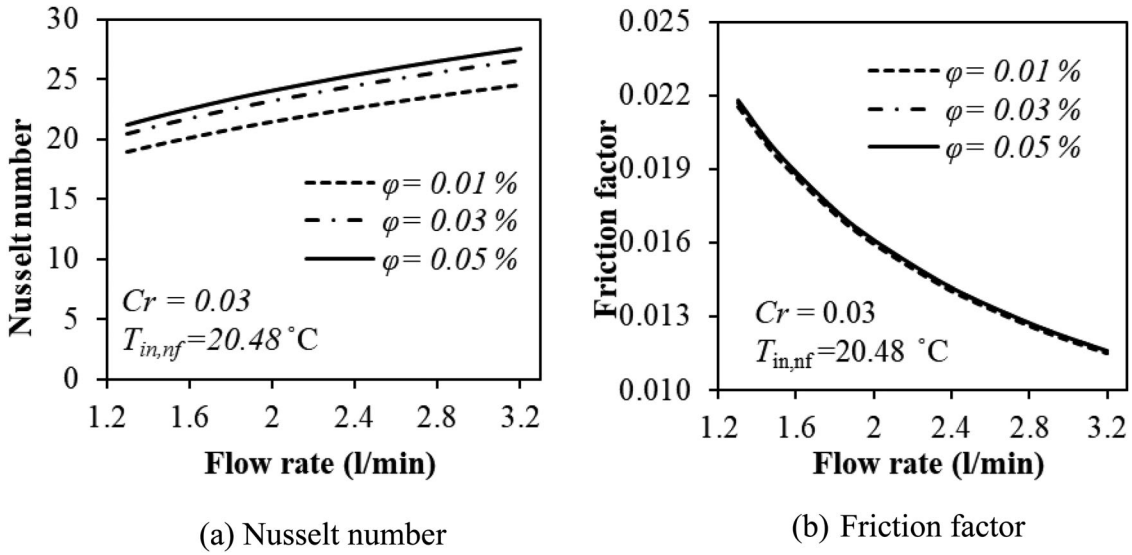

(a) Nusselt number (b) Friction factor

Figure 4. Variation of the (a) Nusselt number and (b) friction factor with flow rate for the different nanoparticle volume fraction.

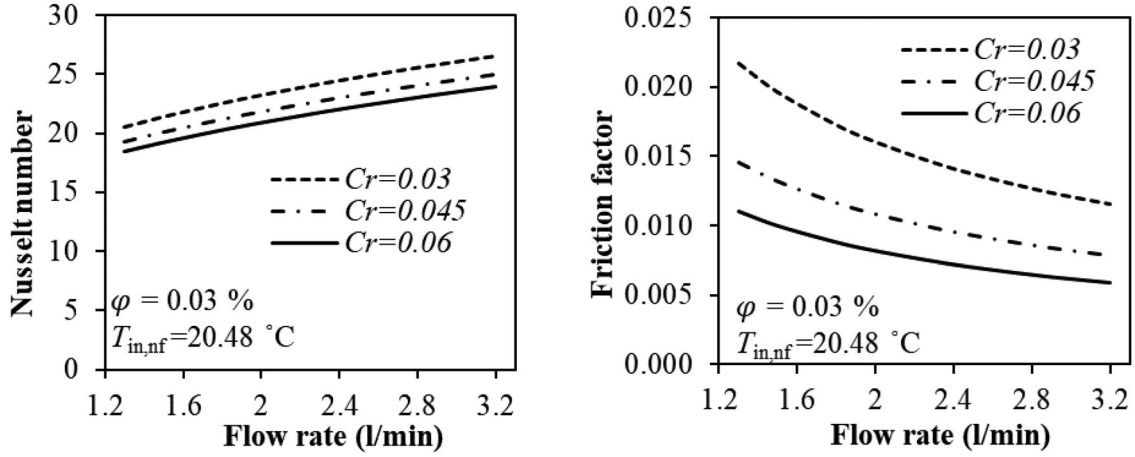

(a) Nusselt number (b) Friction factor

Figure 5. Variation of the (a) Nusselt number and (b) friction factor with flow rate for different curvature ratio.

coil tube with a curvature ratio of 0.03. Increasing the nanoparticle volume fraction intensifies heat transfer in the spiral coil tube, as shown in Figure 4a. The enhanced heat transfer of nanofluid flow in spiral coil tubes can be attributed to the improved thermal properties of nanofluids and cross-sectional mixing due to secondary flow caused by tube curvature, as reported by Doshmanziari et al. [19, 33]. Figure 4b indicates that increasing the nanoparticle volume fraction has a marginal effect on the friction factor in the spiral coil tube. For example, a three-fold increase in the nanoparticle volume fraction (from 0.01% to 0.03%) leads to approximately 8% and only 0.6% growth in the Nusselt number and friction factor, respectively. Jamal-Abad et al. [32] reported similar findings for the effect of the nanoparticle volume fraction on the convective heat transfer of laminar nanofluid flow in spiral coil tubes.

Figure 5 compares the impact of the curvature ratio on the Nusselt number and friction factor of nanofluid flow with 0.03% nanoparticle volume fraction in the spiral coil tube. Decreasing the curvature ratio of spiral coil tubes (increasing the average diameter of the coil) intensifies the secondary flow in coiled tubes, which enhances heat transfer and increases the pressure drop in spiral coil tubes [16, 34, 61, 62]. Figure 5 indicates that the impact of the curvature ratio on the friction factor is more than that of the Nusselt number. For example, a reduction in the curvature ratio, from 0.045 to 0.03, proceeded a 6% and 32.6% increase in the Nusselt number and friction factor, respectively.

Comparing Figures 4 and 5 indicates that the influence of the curvature ratio on the Nusselt number and friction factor of turbulent flow is more significant than that associated with the addition of nanoparticles. Similar results were also reported by Jamal-Abad et al. [32] for laminar nanofluid flow in spiral coil tubes.

Figure 6 illustrates the impact of nanofluid inlet temperature on the heat transfer rate and pressure drop of turbulent nanofluid flow in the spiral coil tube. Decreasing the inlet temperature increases the temperature difference in the heat exchanger, which leads to an enhancement in heat transfer. Reducing the nanofluid inlet temperature proceeds an increase in nanofluid density and viscosity [63], which leads to a rise in the pressure drop. Comparing Figures 6a and 6b indicates that the effect of the inlet temperature drop on the heat transfer rate is more than that of pressure drop. For example, a temperature drop of 3 °C (from 21 °C to 18 °C at $\varphi = 0.03\%$) led to a 14.5% and 3.3% increase in the heat transfer rate and pressure drop, respectively. At a constant temperature, increasing the nanoparticle volume fraction enhances the transport properties of nanofluids [63] – leading to an enhancement in the heat transfer rate as well as pressure drop penalty, as shown in Figure 6.

Entropy generation in the coiled tubes

Figure 7 depicts the influence of the nanoparticle volume fraction on the contribution of the entropy generation due to heat transfer, $(N_s)_T$, and the contribution of the entropy generation caused by the viscous effect, $(N_s)_P$ in spiral coil tubes. It can be observed that $(N_s)_T$ decreases with increasing the nanoparticle volume fraction. Moreover, as mentioned in the previous section and indicated in Figure 4b, the impact of nanoparticle volume fraction on the entropy

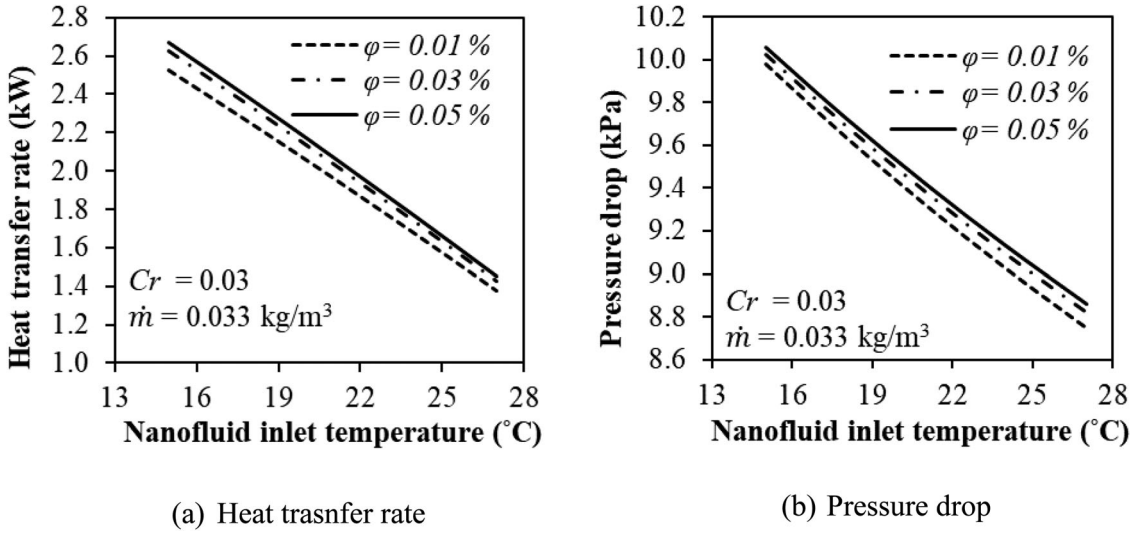

(a) Heat trasnfer rate (b) Pressure drop

Figure 6. Variation of (a) heat transfer rate and (b) pressure drop with nanofluid inlet temperature for different nanoparticle volume fractions.

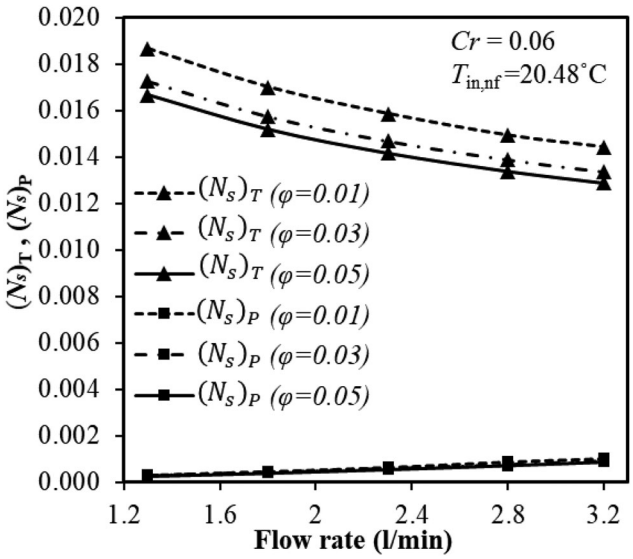

Figure 7. Variation of contributions of the entropy generation number with flow rate for the different nanoparticle volume fraction.

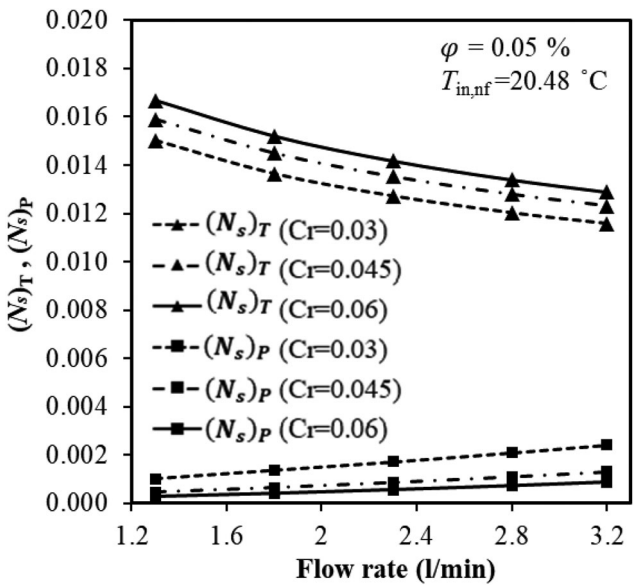

Figure 8. Variation of contributions of the entropy generation number with flow rate for different curvature ratio.

generation caused by the viscous effect is negligible since the nanoparticle volume fraction marginally influences the friction factor. Therefore, increasing the nanoparticle volume fraction declines the total entropy generation in the spiral coil heat exchanger, as indicated in Figure 7. A similar result was reported in a review by Mahian et al. [37] for nanofluid flow in different heat exchangers. Increasing the flow rate enhances the convection heat transfer coefficient which leads to a decrease in $(N_s)_T$, while an augmentation in $(N_s)_p$ is observed with increased flow rate, as shown in Figure 7.

Figure 8 illustrates the effect of the curvature ratio on the contributions of the entropy generation number. Decreasing curvature ratio intensifies secondary flow in the spiral coil tube, leading to heat transfer enhancement and pressure drop penalty. Therefore, reducing the curvature ratio mitigates the irreversibility caused by heat transfer and increases that of due to the viscous effect, as demonstrated in Figure 8.

Figure 9 illustrates the effect of the nanofluid inlet temperature on the contribution of the entropy generation number. Increasing the nanofluid inlet temperature reduces the temperature gap and increases viscous friction (by increasing the viscosity of nanofluid) in the spiral coil tube heat exchanger. Therefore, an increase in the nanofluid inlet temperature reduces the contribution

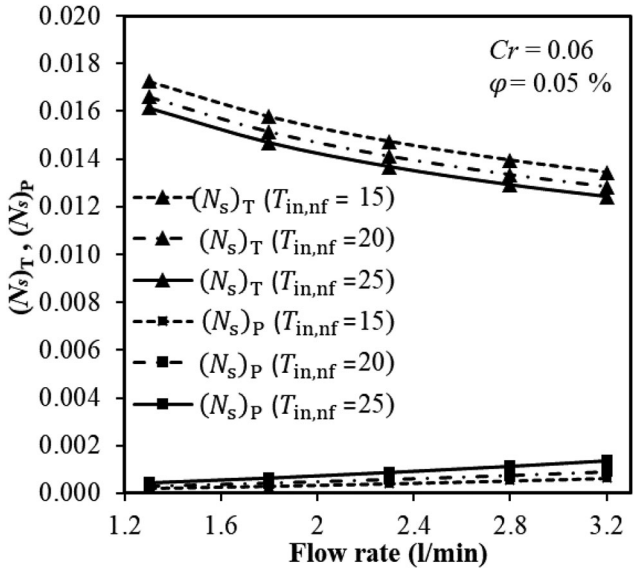

Figure 9. Variation of contributions of the entropy generation number with flow rate for different inlet temperatures.

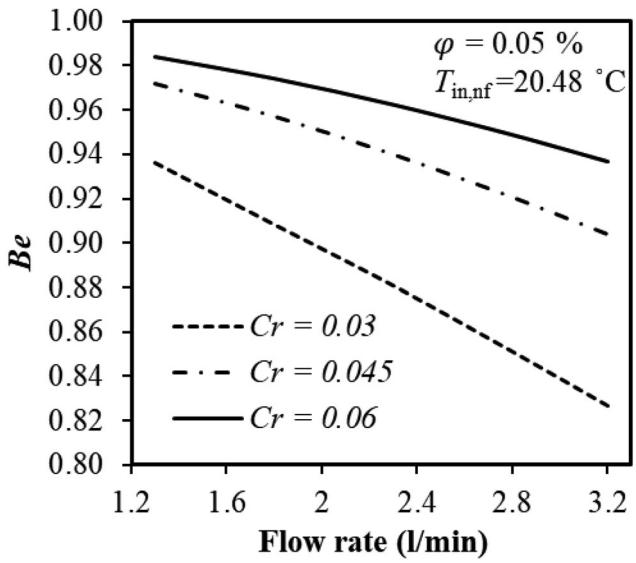

Figure 10. Variation of Bejan number with flow rate for different curvature ratio.

of entropy generation due to heat transfer, while it increases the contribution of entropy generation caused by the viscous effect, as indicated in Figure 9.

Figures 7–9 demonstrate that the contribution of entropy generation due to heat transfer is more than that of the viscous effect. Therefore, reduction of irreversibility caused by heat transfer should be the primary target in the design of spiral coil tubes. For this reason, optimizing the flow parameters and geometry of the spiral coil tube is of significant importance and should be further investigated.

Decreasing the curvature ratio and increasing the inlet temperature reduce the Bejan number, as shown

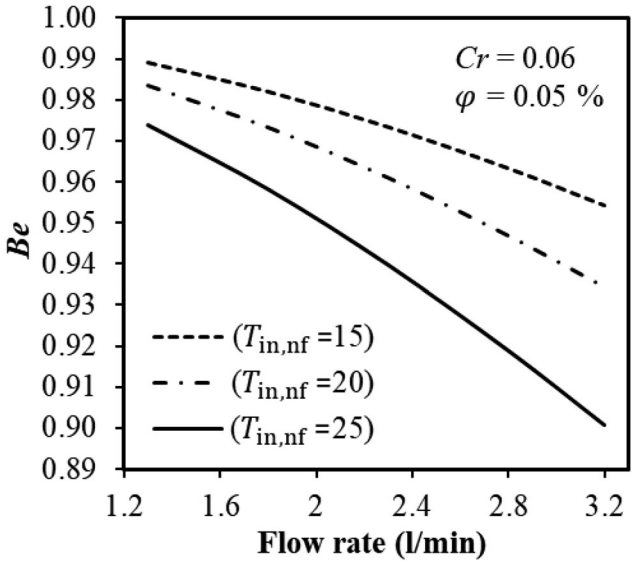

Figure 11. Variation of Bejan number with flow rate for different nanofluid inlet temperature.

in Figures 10 and 11, respectively. Although increasing the inlet temperature reduces the irreversibility (due to the reduction of temperature gap) in the heat exchange, it increases the entropy generation due to viscous effect and reduces heat transfer. On the other hand, reducing the curvature ratio intensifies the secondary flow in the spiral coil tube and enhances the heat transfer coefficient (as shown in Figure 5a). However, decreasing the curvature ratio leads to an increase in the contribution of entropy generation due to the viscous effect (as illustrated in Figure 8). Thus, the curvature ratio of the spiral coil tube could be considered as one of the design parameters for optimization purposes. As shown in Figures 10 and 11, the Bejan number significantly decreases with the flow rate. Therefore, the flow rate (alternatively Reynolds number) can be considered as another design parameter that should be optimized.

Figure 12 depicts the influence of nanofluid inlet temperature, nanoparticle volume fraction, and curvature ratio on the total entropy generation number for different flow rates. At a given inlet temperature and curvature ratio, the total entropy generation number decreased with increasing nanoparticle volume fraction. This means that increasing the nanoparticle volume fraction is always beneficial in the reduction of irreversibility, which agrees with the finding of Mahian et al. [37] and Bianco et al. [38]. For a given flow rate as well as a fixed nanoparticle volume fraction and inlet temperature, reducing the curvature ratio decreased the entropy generation number in the spiral coil tube. This reduction in the entropy generation number, however, diminishes with increasing

the flow rate. Figure 12 shows that for a flow rate of more than 2.8 l/min, decreasing the curvature ratio leads to an increase in the total entropy generation number. For a given nanoparticle volume fraction and fixed curvature ratio, decreasing the nanofluid inlet temperature reduces the total entropy generation number. The impact of inlet temperature reduction on the reduction of the irreversibility at higher flow rates is more than that of lower flow rates, as shown in Figure 12. The total entropy generation number decreases with an increased flow rate, for the range of parameters studied in this paper.

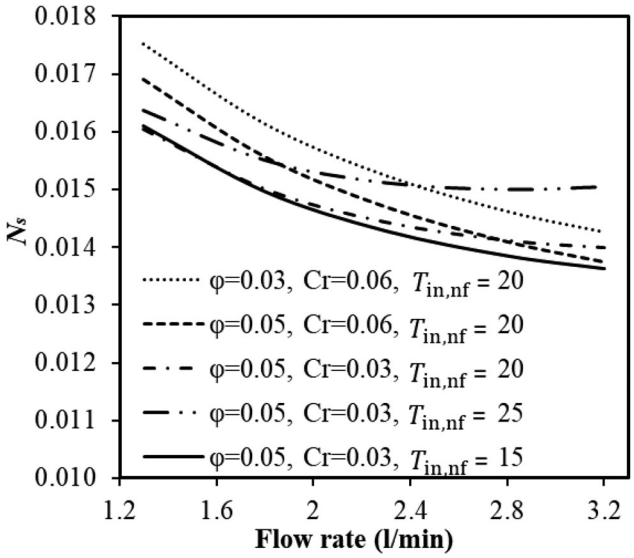

Figure 12. Variation of total entropy generation number with flow rate for a different contributing factor.

Figure 12 demonstrates that the nanoparticle volume fraction, inlet temperature, curvature ratio, and flow rate can significantly influence the total entropy generation in spiral coil tubes. Increasing the nanoparticle volume fraction steadily reduces the total entropy generation. However, an alteration in other parameters can either negatively or positively influence the total entropy generation. The effect of the flow rate, inlet temperature, and nanoparticle volume fraction can be recast to the Reynolds number. Therefore, the Reynolds number and the curvature ratio were considered as design parameters for entropy generation minimization.

Figure 13 illustrates the simultaneous influence of curvature ratio and Reynolds number on the total entropy generation. For a low Reynolds number, decreasing the curvature ratio reduces the total entropy generation. For a high Reynolds number, the total entropy generation significantly increases with decreasing the curvature ratio. However, the total entropy generation shows a marginal sensitivity to the variation of the curvature ratio for a moderate Reynolds number. According to Figure 13, to have an optimum turbulent convective heat transfer, a moderate Reynolds number should be considered in the

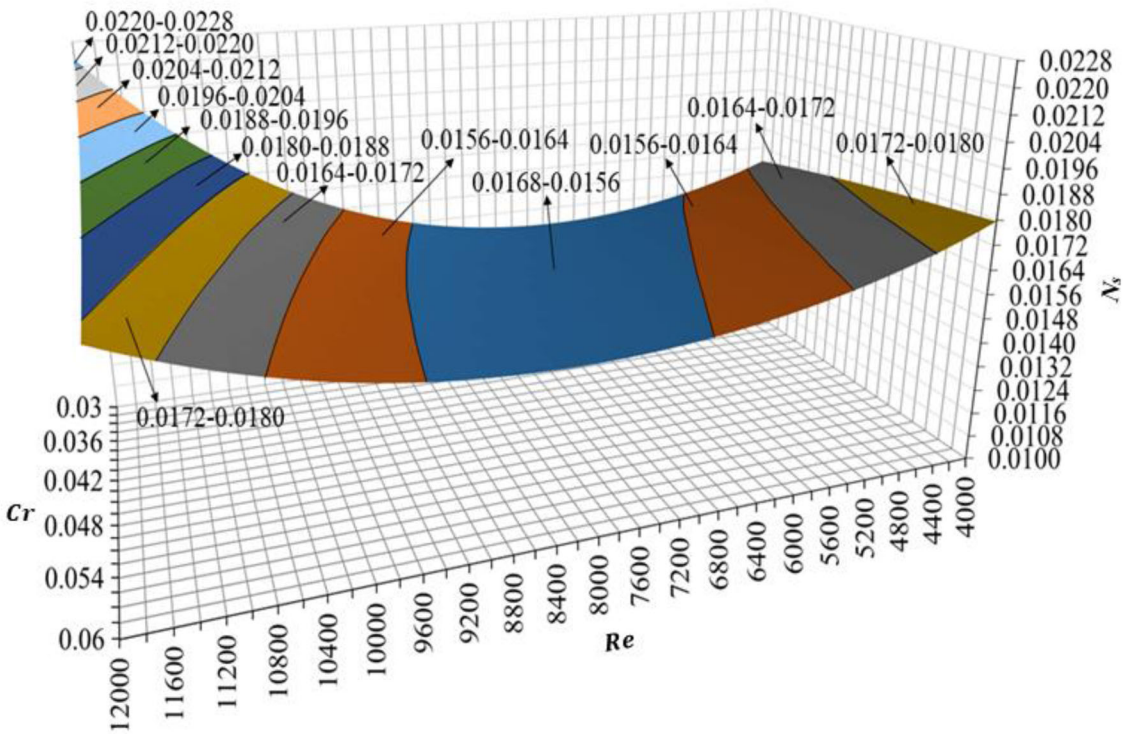

Figure 13. Variation of total entropy generation number with Reynolds number and curvature ratio factor.

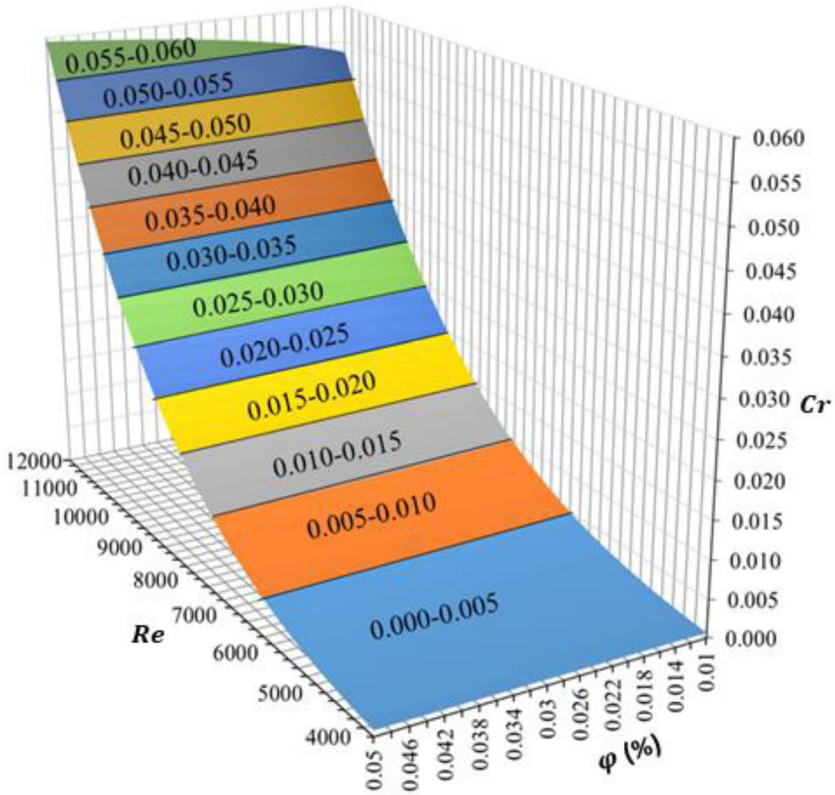

Figure 14. Variation of optimum curvature ratio with Reynolds number and nanoparticle volume fraction ($B_0 = 3 \times 10^{10}$, $Pr = 5$).

design of spiral coil tubes. This result agrees with the finding of Doshmanziari et al. [19].

Thermodynamic optimization

Entropy generation minimization can be performed with respect to either the curvature ratio (to optimize the geometry of the spiral coil tube for a specific flow condition) or the Reynolds number (to optimize the fluid flow condition).

Optimum curvature ratio

For a given duty parameter (B_0) and Prandtl number, the optimum curvature ratio can be calculated from Eq. (17). Figure 14 illustrates the simultaneous influence of the Reynolds number and nanoparticle volume fraction on the optimum curvature ratio of the spiral coil tube. It can be observed that the optimum curvature ratio significantly increases with increased Reynolds number. Thus, to design a compact heat exchanger (a large curvature ratio), a high Reynolds number is favorable. For a low Reynolds number, the nanoparticle volume fraction has a negligible effect on the optimum curvature ratio. For a high Reynolds number, the optimum curvature ratio slightly increases with an augmentation in the nanoparticle volume fraction.

Optimum Reynolds number.

For a given duty parameter (B_0) and Prandtl number, the optimum Reynolds number can be calculated from Eq. (18). For the range of curvature ratio and nanoparticle volume fraction specified in Table 2, an optimum Reynolds number between 9000 and 12000 is desired, as shown in Figure 15. Since the optimum Reynolds number increases with increasing the curvature ratio, a more compact heat exchanger is achievable for higher Reynolds numbers. Increasing the nanoparticle volume fraction leads to a small reduction in the optimum Reynolds number, as shown in Figure 15.

Conclusions

The convection heat transfer and thermodynamic analysis of turbulent TiO_2/water nanofluid flow in the spiral coil tube were performed, and the optimum design parameters were formulated. The following conclusions can be summarized:

- The addition of nanoparticle and decreasing the curvature ratio increased the Nusselt number and pressure drop. However, the influence of the curvature ratio on the Nusselt number and friction factor was more than that associated with the addition of nanoparticles.

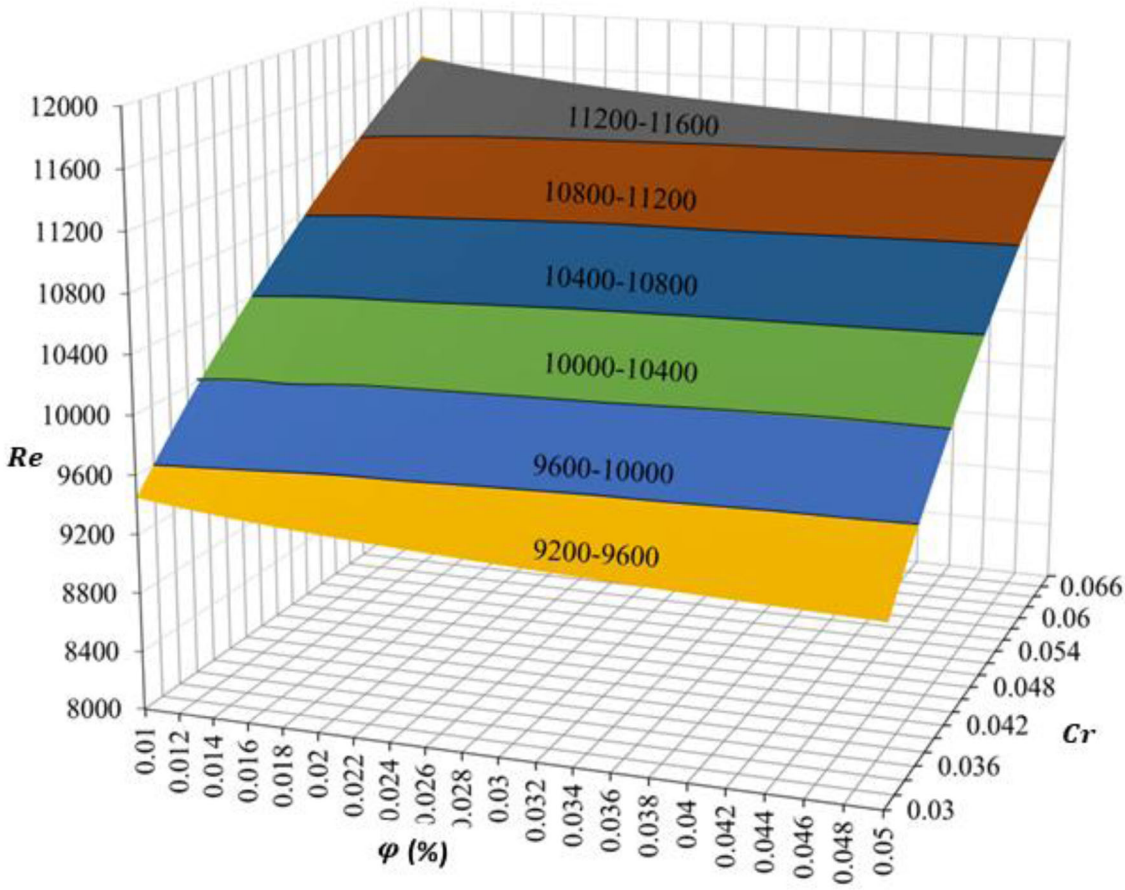

Figure 15. Variation of optimum Reynolds number with curvature ratio and nanoparticle volume fraction ($B_0 = 3 \times 10^{10}$, $Pr = 5$).

- A reduction in the inlet temperature led to an increase in the heat transfer rate and pressure drop, while the influence of the inlet temperature on the heat transfer rate was more than that of pressure drop
- Increasing the nanoparticle volume fraction, flow rate, and inlet temperature as well as reducing the curvature ratio decreased the contribution of entropy generation due to heat transfer. Moreover, increasing the curvature ratio and reducing the flow rate and nanofluid inlet temperature declined the contribution of entropy generation caused by the viscous effect. The variation of the nanoparticle volume fraction had a negligible impact on the contribution of entropy generation produced by the viscous effect.
- The contribution of heat transfer to the entropy generation was more than that of the viscous effect.
- Increasing the nanoparticle volume fraction reduced the total entropy generation. However, reducing of curvature ratio was beneficial for a low Reynolds number and detrimental for a high Reynolds number.
- EGM results showed that an optimum design of spiral coil tube heat exchanger with a high curvature ratio requires a turbulent nanofluid flow with a high Reynolds number. An optimum Reynolds number between 9000 and 12000 was proposed for the range of parameters studied in this paper.
- The impact of nanoparticle volume fraction on the optimum curvature ratio and optimum Reynolds number is marginal.

The findings of this study can be employed for the design and optimization of the turbulent nanofluid flow in the spiral coil tube heat exchangers. The results indicated that higher nanofluid volume fraction could be used for turbulent nanofluid flow in a spiral coil tube with a high curvature ratio. Moreover, there are optimum curvature ratio and Reynolds number associate with the nanofluid flow in spiral coil tubes, which can be evaluated by Eqs. (17) and (18). A high Reynolds number is required in an effort to achieve a compact spiral coil tube heat exchanger with optimum thermal performance. The combination of the economic analysis and the entropy generation minimization method could be considered for future studies.

Disclosure statement

No potential conflict of interest was reported by the authors.

Notes on contributors

Mohammadreza Kadivar received his M.Sc. degree in Mechanical Engineering from Shiraz University, Iran. He is a member of I-Form, Advanced Manufacturing Research Center and also Center for Precision Engineering, Material & Manufacturing Research at the Institute of Technology Sligo, Ireland. He is interested in heat transfer, boiling, computational fluid dynamics, thermal energy storage, and nanofluids. His specific expertise is employing computational, theoretical, and experimental methods to perform research that specifically targets the critical need for improved energy efficiency, storage, transport, and conversion.

Mohsen Sharifpur is an associate professor in the Department of Mechanical and Aeronautical Engineering at the University of Pretoria (UP), South Africa. His research area includes mathematical modeling, improvement of heat transfer by nanofluids, convective multiphase flow, computational fluid dynamics, and fluid dynamics from nanoscale to universe scale. He established a Nanofluid Research Laboratory at UP in 2010, which is one of the most active and productive nanofluids research laboratories in Africa. He is an innovative thinker and based on fluid dynamics, constructal law, nature and patterns in nature, and cosmology data; he invented a new general and multidiscipline theory as "Source and Sink Theory" (https://dx.doi.org/10.22606/tp.2020.51001). His general-multidiscipline theory has the potential to describe the early universe better than previous theories. He believes, his theory is the case of the future. He has authored or coauthored more than 130 peer-reviewed articles and international conference papers.

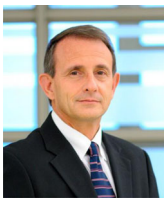

Josua Meyer is a professor, Chair of the School of Engineering and Head of the Department of Mechanical and Aeronautical Engineering at the University of Pretoria, South Africa. He specializes in heat transfer, fluid mechanics and thermodynamic aspects of heating, ventilation, and air-conditioning. He is the author and coauthor of more than 800 articles, conference papers and patents, and has received various prestigious awards for his research. He is also a fellow or member of various professional institutes and societies and is regularly invited as keynote speaker at international conferences. He is the recipient of various teaching awards. He is on the editorial board and/or (lead) editor of 15 journals (including an associate editor of *Heat Transfer Engineering*) and was a member of the scientific committees of more than 40 international conferences, and conference chair of more than 14 international conferences.

References

[1] G. Huminic and A. Huminic, "Heat transfer and flow characteristics of conventional fluids and nanofluids in curved tubes: A review," *Renew. Sustain. Energy Rev.*, vol. 58, pp. 1327–1347, May 2016. DOI: 10.1016/j.rser.2015.12.230.

[2] S. A. Berger, L. Talbot, and L. S. Yao, "Flow in curved pipes," *Annu. Rev. Fluid Mech.*, vol. 15, no. 1, pp. 461–512, Jan. 1983. DOI: 10.1146/annurev.fl.15.010183.002333.

[3] P. Naphon and S. Wongwises, "A review of flow and heat transfer characteristics in curved tubes," *Renew. Sustain. Energy Rev.*, vol. 10, no. 5, pp. 463–490, Oct. 2006. DOI: 10.1016/j.rser.2004.09.014.

[4] S. Vashisth, A. V. Kumar, and K. D. P. Nigam, "A review on the potential applications of curved geometries in process industry," *Ind. Eng. Chem. Res.*, vol. 47, no. 10, pp. 3291–3337, Apr. 2008. DOI: 10.1021/ie701760h.

[5] P. Naphon, S. Wiriyasart, T. Arisariyawong, and T. Nualboonrueng, "Magnetic field effect on the nanofluids convective heat transfer and pressure drop in the spirally coiled tubes," *Int. J. Heat Mass Transfer*, vol. 110, pp. 739–745, Jul. 2017. DOI: 10.1016/j.ijheatmasstransfer.2017.03.077.

[6] Y. Xuan and Q. Li, "Heat transfer enhancement of nanofluids," *Int. J. Heat Fluid Flow*, vol. 21, no. 1, pp. 58–64, Feb. 2000. DOI: 10.1016/S0142-727X(99)00067-3.

[7] A. Kumar and S. Subudhi, "Preparation, characterisation and heat transfer analysis of nanofluids used for engine cooling," *Appl. Therm. Eng.*, vol. 160, pp. 114092, Sep. 2019. DOI: 10.1016/j.applthermaleng.2019.114092.

[8] W. Wang, G. Duan, J. Li, W. Zhao, C. Li, and Z. Liu, "The preparation and thermal performance research of spherical Ag-H2O nanofluids & applied in heat pipe," *Appl. Therm. Eng.*, vol. 116, pp. 811–822, Apr. 2017. DOI: 10.1016/j.applthermaleng.2017.02.018.

[9] T. P. Teng, T. C. Hsiao, and C. C. Chung, "Characteristics of carbon-based nanofluids and their application in a brazed plate heat exchanger under laminar flow," *Appl. Therm. Eng.*, vol. 146, pp. 160–168, Jan. 2019. DOI: 10.1016/j.applthermaleng.2018.09.125.

[10] M. Khoshvaght-Aliabadi and Z. Arani-Lahtari, "Proposing new configurations for twisted square channel (TSC): Nanofluid as working fluid," *Appl. Therm. Eng.*, vol. 108, pp. 709–719, Sep. 2016. DOI: 10.1016/j.applthermaleng.2016.07.173.

[11] M. Malekan, A. Khosravi, and S. Syri, "Heat transfer modeling of a parabolic trough solar collector with working fluid of Fe3O4 and CuO/Therminol 66 nanofluids under magnetic field," *Appl. Therm. Eng.*,

vol. 163, pp. 114435, Dec. 2019. DOI: 10.1016/j.applthermaleng.2019.114435.

[12] S. Chakraborty, I. Sarkar, A. Ashok, I. Sengupta, S. K. Pal, and S. Chakraborty, "Thermo-physical properties of Cu-Zn-Al LDH nanofluid and its application in spray cooling," *Appl. Therm. Eng.*, vol. 141, pp. 339–351, Aug. 2018. DOI: 10.1016/j.applthermaleng.2018.05.114.

[13] Y. Hu, Y. He, H. Gao, and Z. Zhang, "Forced convective heat transfer characteristics of solar salt-based SiO2 nanofluids in solar energy applications," *Appl. Therm. Eng.*, vol. 155, pp. 650–659, Jun. 2019. DOI: 10.1016/j.applthermaleng.2019.04.109.

[14] S. K. Hazra, S. Ghosh, and T. K. Nandi, "Photo-thermal conversion characteristics of carbon black-ethylene glycol nanofluids for applications in direct absorption solar collectors," *Appl. Therm. Eng.*, vol. 163, pp. 114402, Dec. 2019. DOI: 10.1016/j.applthermaleng.2019.114402.

[15] M. Ding, C. Liu, and Z. Rao, "Experimental investigation on heat transfer characteristic of TiO2-H2O nanofluid in microchannel for thermal energy storage," *Appl. Therm. Eng.*, vol. 160, pp. 114024, Sep. 2019. DOI: 10.1016/j.applthermaleng.2019.114024.

[16] X. Zhai, C. Qi, Y. Pan, T. Luo, and L. Liang, "Effects of screw pitches and rotation angles on flow and heat transfer characteristics of nanofluids in spiral tubes," *Int. J. Heat Mass Transfer*, vol. 130, pp. 989–1003, Mar. 2019. DOI: 10.1016/j.ijheatmasstransfer.2018.10.131.

[17] S. Suresh, K. P. Venkitaraj, and P. Selvakumar, "Comparative study on thermal performance of helical screw tape inserts in laminar flow using Al2O3/water and CuO/water nanofluids," *Superlattices Microstruct.*, vol. 49, no. 6, pp. 608–622, Jun. 2011. DOI: 10.1016/j.spmi.2011.03.012.

[18] A. Mokhtari Ardekani, V. Kalantar, and M. M. Heyhat, "Experimental study on heat transfer enhancement of nanofluid flow through helical tubes," *Adv. Powder Technol.*, vol. 30, no. 9, pp. 1815–1822, Sep. 2019. DOI: 10.1016/j.apt.2019.05.026.

[19] F. I. Doshmanziari, M. R. Kadivar, M. Yaghoubi, D. Jalali-Vahid, and M. A. Arvinfar, "Experimental and numerical study of turbulent fluid flow and heat transfer of Al_2O_3/water nanofluid in a spiral-coil tube," *Heat Transfer Eng.*, vol. 38, no. 6, pp. 611–626, Apr. 2017. DOI: 10.1080/01457632.2016.1200380.

[20] M. Karami, M. A. Akhavan-Behabadi, and M. Fakoor-Pakdaman, "Heat transfer and pressure drop characteristics of nanofluid flows inside corrugated tubes," *Heat Transfer Eng.*, vol. 37, no. 1, pp. 106–114, Jan. 2016. DOI: 10.1080/01457632.2015.1042347.

[21] R. M. Moghari, F. Talebi, R. Rafee, and M. Shariat, "Numerical study of pressure drop and thermal characteristics of Al_2O_3-water nanofluid flow in horizontal annuli," *Heat Transfer Eng.*, vol. 36, no. 2, pp. 166–177, Jan. 2015. DOI: 10.1080/01457632.2014.909193.

[22] R. Saxena, D. Gangacharyulu, and V. K. Bulasara, "Heat transfer and pressure drop characteristics of dilute alumina–water nanofluids in a pipe at different power inputs," *Heat Transfer Eng.*, vol. 37, no. 18, pp. 1554–1565, Dec. 2016. DOI: 10.1080/01457632.2016.1151298.

[23] D. Mansoury, F. I. Doshmanziari, A. Kiani, A. J. Chamkha, and M. Sharifpur, "Heat transfer and flow characteristics of Al2O3/water nanofluid in various heat exchangers: Experiments on counter flow," *Heat Transfer Engineering*, vol. 41, no. 3, pp. 220–234, 2020. DOI: 10.1080/01457632.2018.1528051.

[24] A. Bejan, "A study of entropy generation in fundamental convective heat transfer," *J. Heat Transfer*, vol. 101, no. 4, pp. 718–725, Nov. 1979. DOI: 10.1115/1.3451063.

[25] A. Bejan, *Entropy Generation through Heat and Fluid Flow*. New York, NY, USA John Wiley & Sons, 1982.

[26] A. Bejan, "Second law analysis in heat transfer," *Energy*, vol. 5, no. 8–9, pp. 720–732, Aug. 1980. DOI: 10.1016/0360-5442(80)90091-2.

[27] A. Bejan, "Entropy generation minimisation: The new thermodynamics of finite-size devices and finite-time processes," *J. Appl. Phys.*, vol. 79, no. 3, pp. 1191–1218, Feb. 1996. DOI: 10.1063/1.362674.

[28] A. Bejan, "Fundamentals of exergy analysis, entropy generation minimisation, and the generation of flow architecture," *Int. J. Energy Res.*, vol. 26, no. 7, pp. 0–546, Jun. 2002. DOI: 10.1002/er.804.

[29] A. Sciacovelli, V. Verda, and E. Sciubba, "Entropy generation analysis as a design tool—A review," *Renew. Sustain. Energy Rev.*, vol. 43, pp. 1167–1181, Mar. 2015. DOI: 10.1016/j.rser.2014.11.104.

[30] A. Bejan, "General criterion for rating heat-exchanger performance," *Int. J. Heat Mass Transfer*, vol. 21, no. 5, pp. 655–658, May 1978. DOI: 10.1016/0017-9310(78)90064-9.

[31] A. Sasmito, J. Kurnia, and A. Mujumdar, "Numerical evaluation of laminar heat transfer enhancement in nanofluid flow in coiled square tubes," *Nanoscale Res. Lett.*, vol. 6, no. 1, pp. 376–314, 2011. DOI: 10.1186/1556-276X-6-376.

[32] M. T. Jamal-Abad, A. Zamzamian, and M. Dehghan, "Experimental studies on the heat transfer and pressure drop characteristics of Cu–water and Al–water nanofluids in a spiral coil," *Exp. Therm. Fluid Sci.*, vol. 47, pp. 206–212, May 2013. DOI: 10.1016/j.expthermflusci.2013.02.001.

[33] F. I. Doshmanziari, A. E. Zohir, H. R. Kharvani, D. Jalali-Vahid, and M. R. Kadivar, "Characteristics of heat transfer and flow of Al2O3/water nanofluid in a spiral-coil tube for turbulent pulsating flow," *Heat Mass Transfer*, vol. 52, no. 7, pp. 1305–1320, Jul. 2016. DOI: 10.1007/s00231-015-1651-y.

[34] P. Naphon, "Experimental investigation the nanofluids heat transfer characteristics in horizontal spirally coiled tubes," *Int. J. Heat Mass Transfer*, vol. 93, pp. 293–300, Feb. 2016. DOI: 10.1016/j.ijheatmasstransfer.2015.09.089.

[35] P. Naphon, T. Arisariyawong, and T. Nualboonrueng, "Nanofluids heat transfer and flow analysis in vertical spirally coiled tubes using Eulerian two-phase turbulent model," *Heat Mass Transfer*, vol. 53, no. 7, pp. 2297–2308, Jul. 2017. DOI: 10.1007/s00231-017-1977-8.

[36] P. Naphon and S. Wiriyasart, "Pulsating TiO2/water nanofluids flow and heat transfer in the spirally coiled tubes with different magnetic field directions," *Int. J. Heat Mass Transfer*, vol. 115, pp. 537–543, Dec. 2017. DOI: 10.1016/j.ijheatmasstransfer.2017.07.080.

[37] O. Mahian *et al.*, "A review of entropy generation in nanofluid flow," *Int. J. Heat Mass Transfer*, vol. 65, pp. 514–532, Oct. 2013. DOI: 10.1016/j.ijheatmasstransfer.2013.06.010.

[38] V. Bianco, S. Nardini, and O. Manca, "Enhancement of heat transfer and entropy generation analysis of nanofluids turbulent convection flow in square section tubes," *Nanoscale Res. Lett.*, vol. 6, no. 1, pp. 252, Mar. 2011. DOI: 10.1186/1556-276X-6-252.

[39] M. Moghaddami, A. Mohammadzade, and S. A. V. Esfehani, "Second law analysis of nanofluid flow," *Energy Convers. Manage.*, vol. 52, no. 2, pp. 1397–1405, Feb. 2011. DOI: 10.1016/j.enconman.2010.10.002.

[40] M. Moghaddami, S. Shahidi, and M. Siavashi, "Entropy generation analysis of nanofluid flow in turbulent and laminar regimes," *J. Comp. Theor. Nanosci.*, vol. 9, no. 10, pp. 1586–1595, Oct. 2012. DOI: 10.1166/jctn.2012.2249.

[41] K. Y. Leong, R. Saidur, T. M. I. Mahlia, and Y. H. Yau, "Entropy generation analysis of nanofluid flow in a circular tube subjected to constant wall temperature," *Int. Commun. Heat Mass Transfer*, vol. 39, no. 8, pp. 1169–1175, Oct. 2012. DOI: 10.1016/j.icheatmasstransfer.2012.06.009.

[42] M. Farzaneh-Gord, H. Ameri, and A. Arabkoohsar, "Tube-in-tube helical heat exchangers performance optimisation by entropy generation minimisation approach," *Appl. Therm. Eng.*, vol. 108, pp. 1279–1287, Sep. 2016. DOI: 10.1016/j.applthermaleng.2016.08.028.

[43] M. Ahadi and A. Abbassi, "Exergy analysis of laminar forced convection of nanofluids through a helical coiled tube with uniform wall heat flux," *IJEX Int. J. Exergy*, vol. 13, no. 1, pp. 21–15, 2013. DOI: 10.1504/IJEX.2013.055776.

[44] A. Zamzamian, "Entropy generation analysis of EG – Al2O3 nanofluid flows through a helical pipe," *Int. J. Nanosci. Nanotechnol.*, vol. 10, no. 2, pp. 103–110, Jun. 2014.

[45] A. Falahat, "Entropy generation analysis of EG-Al_2O_3 nanofluid in helical tube and laminar flow," *Int. J. Multidiscipl. Sci. Eng.*, vol. 2, no. 7, pp. 44–47, Oct. 2011.

[46] G. Huminic and A. Huminic, "Heat transfer and entropy generation analyses of nanofluids in helically coiled tube-in-tube heat exchangers," *Int. Commun. Heat Mass Transfer*, vol. 71, pp. 118–125, Feb. 2016. DOI: 10.1016/j.icheatmasstransfer.2015.12.031.

[47] G. Huminic and A. Huminic, "Heat transfer characteristics in double tube helical heat exchangers using nanofluids," *Int. J. Heat Mass Transfer*, vol. 54, no. 19–20, pp. 4280–4287, Sep. 2011. DOI: 10.1016/j.ijheatmasstransfer.2011.05.017.

[48] H. Khosravi-Bizhaem and A. Abbassi, "Effects of curvature ratio on forced convection and entropy generation of nanofluid in helical coil using two-phase approach," *Adv. Powder Technol.*, vol. 29, no. 4, pp. 890–903, Apr. 2018. DOI: 10.1016/j.apt.2018.01.005.

[49] L. Yang and K. Du, "A comprehensive review on heat transfer characteristics of TiO2 nanofluids," *Int. J. Heat Mass Transfer*, vol. 108, pp. 11–31, May 2017. DOI: 10.1016/j.ijheatmasstransfer.2016.11.086.

[50] M. A. Khairul, R. Saidur, M. M. Rahman, M. A. Alim, A. Hossain, and Z. Abdin, "Heat transfer and thermodynamic analyses of a helically coiled heat exchanger using different types of nanofluids," *Int. J. Heat Mass Transfer*, vol. 67, pp. 398–403, Dec. 2013. DOI: 10.1016/j.ijheatmasstransfer.2013.08.030.

[51] T. H. Ko and K. Ting, "Entropy generation and thermodynamic optimisation of fully developed laminar convection in a helical coil," *Int. Commun. Heat Mass Transfer*, vol. 32, no. 1–2, pp. 214–223, Jan. 2005. DOI: 10.1016/j.icheatmasstransfer.2004.04.039.

[52] A. Bejan, "Second-law analysis in heat transfer and thermal design," *Adv. Heat Transfer*, vol. 15, pp. 1–58, Jan. 1982. DOI: 10.1016/S0065-2717(08)70172-2..

[53] H. K. Bizhaem and A. Abbassi, "Numerical study on heat transfer and entropy generation of developing laminar nanofluid flow in helical tube using two-phase mixture model," *Adv. Powder Technol.*, vol. 28, no. 9, pp. 2110–2125, Sep. 2017. DOI: 10.1016/j.apt.2017.05.018.

[54] O. Mahian, A. Kianifar, S. Z. Heris, and S. Wongwises, "Natural convection of silica nanofluids in square and triangular enclosures: Theoretical and experimental study," *Int. J. Heat Mass Transfer*, vol. 99, pp. 792–804, Aug. 2016. DOI: 10.1016/j.ijheatmasstransfer.2016.03.045.

[55] B. C. Pak and Y. I. Cho, "Hydrodynamic and heat transfer study of dispersed fluids with submicron metallic oxide particles," *Exp. Heat Transfer*, vol. 11, no. 2, pp. 151–170, Apr. 1998. DOI: 10.1080/08916159808946559.

[56] M. Corcione, "Heat transfer features of buoyancy-driven nanofluids inside rectangular enclosures differentially heated at the sidewalls," *Int. J. Therm. Sci.*, vol. 49, no. 9, pp. 1536–1546, Sep. 2010. DOI: 10.1016/j.ijthermalsci.2010.05.005.

[57] A. A. Abbasian Arani and J. Amani, "Experimental study on the effect of TiO2–water nanofluid on heat transfer and pressure drop," *Exp. Therm. Fluid Sci.*, vol. 42, pp. 107–115, Oct. 2012. DOI: 10.1016/j.expthermflusci.2012.04.017.

[58] A. R. Sajadi and M. H. Kazemi, "Investigation of turbulent convective heat transfer and pressure drop of TiO2/water nanofluid in circular tube," *Int. Commun. Heat Mass Transfer*, vol. 38, no. 10, pp. 1474–1478, Dec. 2011. DOI: 10.1016/j.icheatmasstransfer.2011.07.007.

[59] R. V. Pinto and F. A. S. Fiorelli, "Review of the mechanisms responsible for heat transfer enhancement using nanofluids," *Appl. Therm. Eng.*, vol. 108, pp. 720–739, Sep. 2016. DOI: 10.1016/j.applthermaleng.2016.07.147.

[60] M. M. Heyhat and F. Kowsary, "Effect of particle migration on flow and convective heat transfer of

nanofluids flowing through a circular pipe," *J. Heat Transfer*, vol. 132, no. 6, pp. 062401, Jun. 2010. DOI: 10.1115/1.4000743.

[61] R. H. Patil, "Experimental studies on heat transfer to Newtonian fluids through spiral coils," *Exp. Therm. Fluid Sci.*, vol. 84, pp. 144–155, Jun. 2017. DOI: 10.1016/j.expthermflusci.2017.02.002.

[62] P. Naphon and J. Suwagrai, "Effect of curvature ratios on the heat transfer and flow developments in the horizontal spirally coiled tubes," *Int. J. Heat Mass Transfer*, vol. 50, no. 3–4, pp. 444–451, Feb. 2007. DOI: 10.1016/j.ijheatmasstransfer.2006.08.002.

[63] O. Mahian *et al.*, "Recent advances in modeling and simulation of nanofluid flows-Part I: Fundamentals and theory," *Phys. Rep.*, vol. 790, pp. 1–48, Feb. 2019. DOI: 10.1016/j.physrep.2018.11.004.

Appendix: "Trial and error" for calculating the average bulk temperature of the nanofluid

At a given temperature of the hot water storage, T_h, and nanofluid inlet temperature, $T_{in,nf}$, with an initial guess of nanofluid outlet temperature, $T_{out,nf,i}$, the logarithmic mean temperature difference of the nanofluid can be calculated by

$$\Delta T_{LMTD} = \frac{(T_h - T_{in,nf}) - (T_h - T_{out,nf,i})}{\ln\left(\frac{T_h - T_{in,nf}}{T_h - T_{out,nf,i}}\right)} \tag{A1}$$

Moreover, the thermophysical properties of nanofluid can be calculated by the relations provided in this paper at the average bulk nanofluid temperature of $T_b = (T_{in,nf} + T_{out,nf,i})/2$. By knowing the thermophysical properties, the Nusselt number can be calculated by Eq. (14). Consequently, the absorbed heat by nanofluid is calculated by

$$Q_{nf} = \frac{Nu\ k_{nf}}{D} A_s\ \Delta T_{LMTD} \tag{A2}$$

where A_s is the inside heat transfer area of the spiral coil. The outlet temperature of nanofluid is calculated by

$$T_{out,nf} = T_{in,nf} + \frac{Q_{nf}}{\dot{m}_{nf} C_{p_{nf}}} \tag{A3}$$

where $\dot{m}_{nf}$ is the nanofluid mass flow rate. The nanofluid outlet temperature, $T_{out,nf}$, can be used as a next guess to repeat the procedure until the criterion of $T_{out,nf} - T_{out,nf,i} < \varepsilon$ reaches. In this study, $\varepsilon = 0.00001$ was considered.